CERAMICS — Silikáty 34, s. 315—330 (1990)

THE MINERAL GYROLITE AND ITS STABILITY UNDER HYDROTHERMAL CONDITIONS

LADISLAV ŠTEVULA, MIROSLAV HARMAN*, IVAN HORVÁTH, KAROL PUTYERA

Institute of Inorganic Chemistry, Centre of Chemical Research, Slovak Academy of Sciences, Dúbravská cesta, 842 36 Bratislava

**Geological Institute of the Centre of Geological Scientific Research, Slovak Academy of Sciences, Dúbravská cesta 814 73*

Received 15. 9. 1989

The effect of temperature under hydrothermal conditions on the stability of the natural mineral gyrolite (in association with laumontite) and synthetic gyrolite was studied. The initial materials as well as the final products were identified by X-ray diffractography, further characteristics were determined by thermal analysis, IR spectroscopy and electron scanning microscopy. It was found that over the temperature range of 200 to 300 °C under hydrothermal conditions, both the natural and synthetic gyrolite behave analogously. At 200 °C and under pressure of saturated water vapour, gyrolite and laumonite can coexist in natural specimens owing to similar CaO/SiO_2 ratios. Above this temperature (at about 220 °C and higher) the laumontite remains stable whereas gyrolite decomposes, producing the stable hydrates truscottite and xonotlite.

INTRODUCTION

During geological surveys of rocks in the so-called Tatiar intrusive complex (between the villages Rudno-Brehy-Pukanec in the western part of the Kremnice-Štiavnica mountainrange in Slovakia) the fissure occupation in granodioritic porphyries was found to contain the zeolitic mineral laumontite ($CaAl_2Si_4O_{12} . 4 H_2O$) in association with a white fine-grained mineral, non-uniformly dispersed among the crystals of laumontite, calcite and quartz, on *X*-ray diffraction patterns exhibiting strong peaks with interplanar distances of 2.2 and 1.1 nm. Harman et al. [1] identified this mineral as gyrolite (hydrated calcium silicate), having the chemical composition $Ca_{16}Si_{24}O_{60}(OH)_8 . 12 H_2O$.

This is the first discovery of natural gyrolite in Slovakia. The occurence of gyrolite in nature has so far been described only sporadically. In Bohemia, gyrolite was found in the south-east surroundings of Česká Lípa in the localities of Jakuby, Srní and Provodín [2], where it occurs in fissure occupation in basalts in association with zeolitic minerals.

Gyrolite is a subject of considerable interest for mineralogists as well as chemists, namely from the standpoint of the reactions in the system $CaO—SiO_2—H_2O$ under hydrothermal conditions. The previous studies were mainly concerned with the structure, crystallochemistry and stability of gyrolite in relation to its analogies truscottite and reyerite.

The present paper is concerned with comparing the stability of the natural mineral gyrolite in association with laumontite, with that of synthetic gyrolite under hydrothermal conditions over the temperature range of 200 to 300 °C.

THEORETICAL

The structure and crystallochemistry of gyrolite, truscottite and reyerite.

The structure, optical properties and chemistry of natural gyrolite were studied by Mackay and Taylor [3], Chalmers et al. [4], Merlino [5], Gard et al. [6] and Lachowski et al. [7]. The authors found that the minerals of the group have a laminar structure in which octahedral and tetrahedral lattices (with tetrahedraly coordinated Si atoms and octahedrally coordinated Ca atoms) are alternated with an interlayer lattice of octahedrally coordinated Ca atoms and water molecules. The ideal crystallochemical formula of gyrolite, $Ca_{16}Si_{24}O_{60}(OH)_8 \cdot (14+x)H_2O$ can also be written in the form $[Ca_{14}(Si_8O_{20}) \cdot (Si_8O_{20})_2 (OH)_8]^{4-} \cdot [Ca_2(H_2O)_8 \cdot (6+x) H_2O]^{4+}$, which shows that the tetrahedral lattice consists of structural $(Si_8O_{20})^{8-}$ units, the octahedral lattice of structural units $Ca_{14}O_{20}(OH)_8^{20-}$ and the composition of the interlayer lattice in the structural unit of gyrolite represents $[Ca_2(H_2O)_8 \cdot (6+x) H_2O]^{4+}$.

The structural unit of reyerite, having the composition $[(Na, K)_2Ca_{14}Si_{22}Al_2O_{58}(OH)_8 \cdot 6 H_2O]$ is remarkable by the presence of two types of tetrahedral layers: one is composed of anions $Si_8O_{20}^{8-}$ and the other containing the anions of $Si_{14}Al_2O_{38}^{14-}$.

The third member of the group of isostructural minerals being discussed, truscottite, has the crystallochemical formula $Ca_{14}Si_{24}O_{58}(OH)_8 \cdot 2 H_2O$.

Hydrothermal synthesis and stability of gyrolite in the system $CaO—SiO_2—H_2O$

The synthesis of phases in the system $CaO—SiO_2—H_2O$ under hydrothermal conditions at 200 to 300 °C was described by Taylor [8]. Gyrolite can be synthetized from CaO and various forms of SiO_2 (such as silicic acid, silica glass, SiO_2 gel, quartz) with the molar ratio $CaO/SiO_2 = 0.66$ in aqueous suspension at temperatures of about 200 °C. The phase composition of the hydrates in the given system depends on the CaO/SiO_2 ratio chosen, the character and properties of the silicic oxide employed, as well as on the temperature and duration of the hydrothermal process. Kalousek and Nelson [9], and also Ševula and Petrovič [10] found that gyrolite can likewise be prepared by interacting dicalcium silicate ($2 CaO \cdot SiO_2$) with SiO_2 in aqueous suspension under hydrothermal conditions.

At a molar ratio $CaO/SiO_2 = 0.50$ and 0.66 in the system $CaO—SiO_2—H_2O$, under hydrothermal conditions over the temperature range of 200 to 300 °C and under saturated water vapour pressure, as well as under high pressures of the liquid, there exist the stable phases of truscottite and gyrolite. Their formation, stability and phase relationship were studied in detail and plotted in phase equilibrium diagrams (Figs 1 through 3) by Roy and Harker [11], Harker [12] and Taylor [8]. Fig. 1 shows that at 200 °C and under relatively high liquid pressures, gyrolite and SiO_2 are stable phases up to about 210 °C on the connecting line between gyrolite and SiO_2. Above this temperature, tobermorite becomes more stable whereas the gyrolitic phase on the gyrolite — xonotlite connecting line is becoming unstable. Fig. 2 indicates that at 250 °C (under more than 100 MPa) the gyrolite-SiO_2 mixture already reacts, producing truscottite $+H_2O$ or gyrolite;

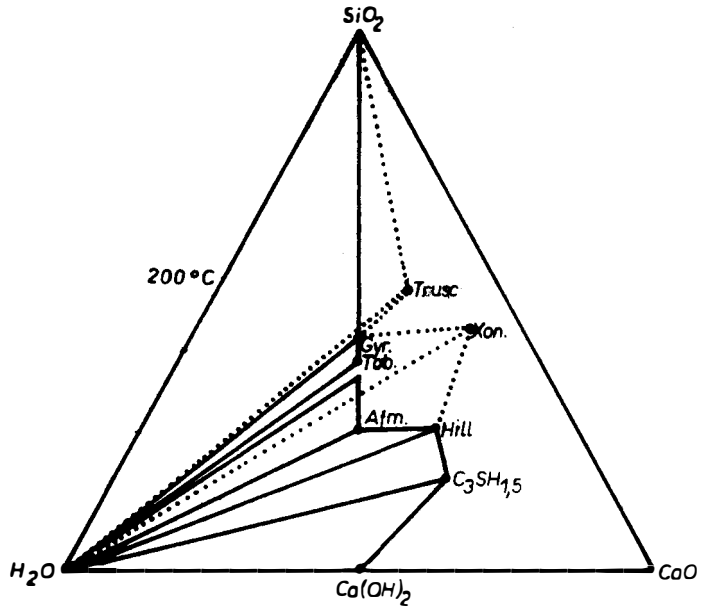

Fig. 1. Equilibrium phase diagram in the system CaO—SiO_2—H_2O *undser hydrothermal conditions at 200 °C.*

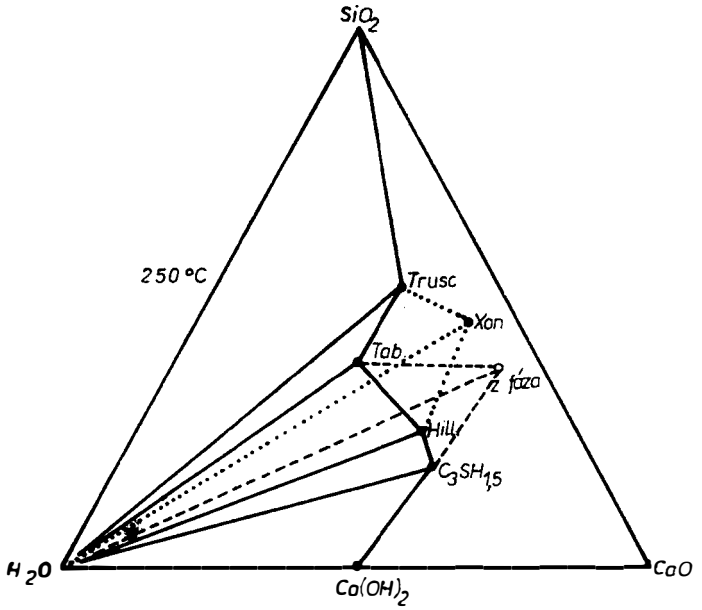

Fig. 2. Equilibrium phase diagram in the system CaO—SiO_2—H_2O *under hydrothermal conditions at 250 °C.*

the latter decomposes as a separate phase, producing truscottite and tobermorite. Tobermorite is decomposed at 300 °C (Fig. 3), and xonotlite and truscottite become stable phases over a wide pressure range of up to 200 MPa.

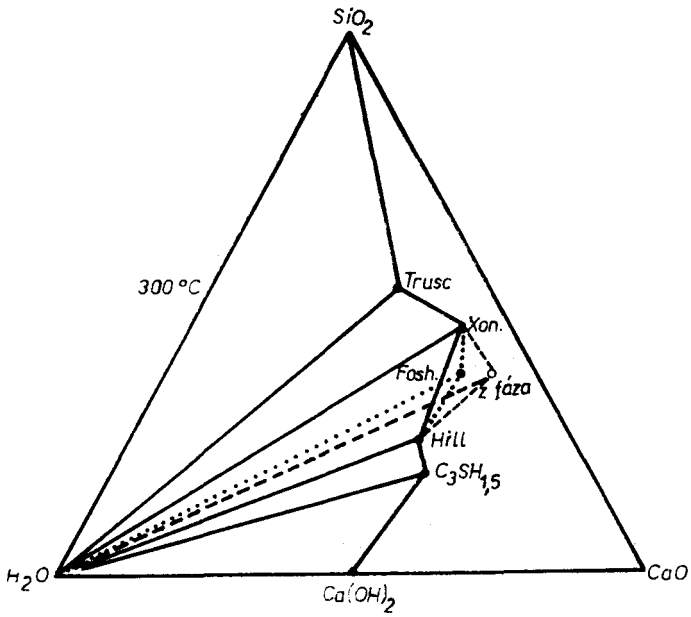

Fig. 3. Equilibrium phase diagram in the system CaO—SiO_2—H_2O *under hydrothermal conditions at 300 °C.*

EXPERIMENTAL

Initial materials

Natural gyrolite

Natural gyrolite was found in samples taken from boreholes in the Banisko locality (hole V-4, 490 m and V-6, 484 m). Sample V-4 (490 m) represents a light-grey granodiorite porphyry with a massive texture. Sample V-6 (484 m) is a granodioritic porphyry with distinct phenocrysts of dark minerals. Gyrolite jointly with laumontite occur in fissure occupation of these rocks, where they form a fine-grained white or light-grey mass jointly with calcite and quartz. The size of the fissures represents several millimetres.

Synthetic gyrolite and synthetic truscottite

The synthesis was made using the molar ratio $CaO/SiO_2 = 0.66$ for gyrolite and 0.50 for truscottite. The CaO was prepared by ignition of $CaCO_3$ A.R. at 1000 °C for 3 hours. Silica colloidal powder BDH was used as a source of SiO_2. The mixtures of homogenized components in aqueous suspension (the ratio water: solid phase =

= 10 : 1) in covered Pt crucibles were subjected to hydrothermal treatment in small stainless steel cylinders at 200, 250 and 300 °C for 7 days. The products obtained were dried at 105 °C.

The research methods used

The phase composition of the specimens was identified by means of *X*-ray diffraction phase analysis of non-oriented powdered samples (diffractometer Philips, CuK α radiation, Ni-filter, 40 kV, 20 mA). The thermal analyses were carried out on Derivatograph Q-1500 and the DuPont 990 thermoanalyzer (TGA thermobalance at a heating rate of 20 °C min^{-1}, sample weight 12—15 mg, N_2 atmosphere at a rate of flow of 1 cm^3 s^{-1}, and DSC module at a heating rate of 10 °C min^{-1}, sample weight 8—10 mg, atmosphere of flowing N_2).

The IR spectra were obtained by means of the Perkin—Elmer 983 G spectrometer over the range of 4000—300 cm^{-1} (pellets of 100 mg KBr, 0.2 mg of sample). Characteristics of the IR spectra of the specimens were compared with tabulated values.

The morphological properties of the samples, the shape of the individual crystals and their habitus were investigated by means of the Tesla BS 300 electron scanning microscope on natural fracture surfaces. The synthetic samples were studied in the form of a settled suspension on a pad. The specimens were metallized with gold.

RESULTS AND DISCUSSION

Mineralogical characteristics of the natural sample

Table I shows the results of *X*-ray diffraction phase analysis of the natural and synthetic minerals compared with the tabulated values of interplanar distances [13, 14, 15, 16, 17, 18, 19]. The presence of gyrolite in natural samples is indicated

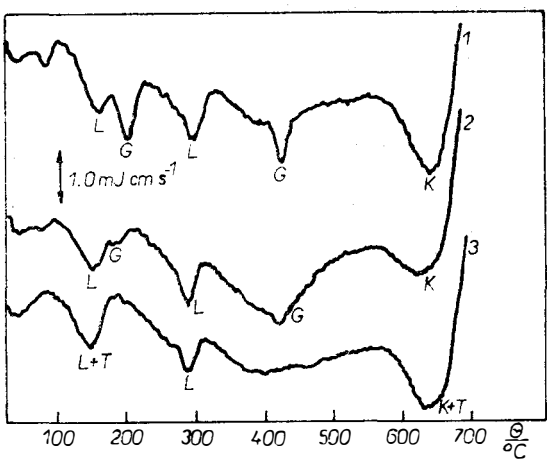

Fig. 4. DSC curves of an aqueous suspension of the natural sample after hydrothermal treatment at 200 °C (curve 1), 250 °C (curve 2) and 300 °C (curve 3).

particularly by basal diffractions in the range of 2.2 and 1.1 nm. Also other diffractions of gyrolite were established at 0.75, 0.47, 0.42, 0.38, 0,34, 0.242 and 0.232 nm.

Apart from gyrolite, the natural samples also evidently contained laumontite with diffraction in the regions of 0.94, 0.68, 0.415, 0.366, 0.349, 0.332 nm, and others. A distinct diffraction at 0.302 nm corresponds to calcite. *X*-ray diffraction patterns indicate that minute admixtures of truscottite as well as of zeolitic minerals stilbite and clinoptilolite cannot be ruled out apart from the gyrolite and laumontite as the main components.

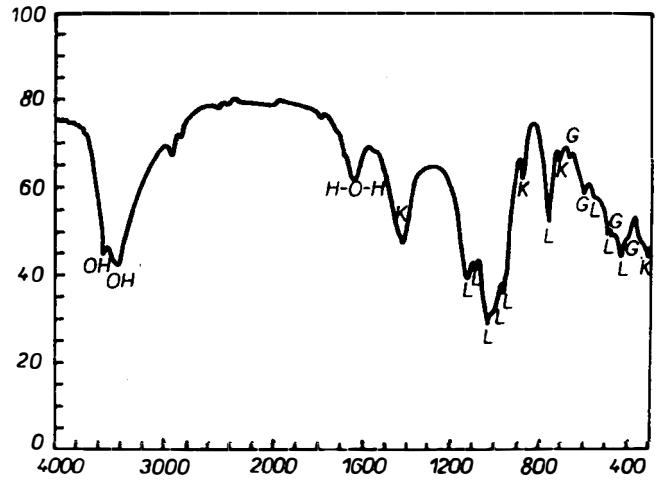

Fig. 5. IR absorption spectrum of the sample of natural gyrolite with laumontite.

The infra-red absorption spectrum of the mineral, designated V-4 (Fig. 5) showed the presence of gyrolite according to the characteristic bands at wavelengths of 390, 465, 480, 500, 600, 675, 785, 1000, 1030 and 1125 cm^{-1}. Laumontite exhibits characteristic bands at 432, 492, 525, 565, 765, 960, 1000, 1060 and 1134 cm^{-1}. The additional bands correspond mainly to calcite and quartz.

Gyrolite in the natural sample was also characterized by studying the morphology of its crystals using electron scanning microscopy (Figs. 6 and 7). Unlike laumontite which forms long prismatic to rod-shaped crystals, gyrolite forms tabular pseudohexagonal crystals up to 6 μm in size and to 1 μm in thickness, with a distinct cleavage in the direction of basal planes. The microscopic investigation also indicates that the gyrolite crystals are intergrown with those of laumontite, or in some cases ingrown into the planes of prismatic laumontite crystas (Fig. 8). To compare the morphology of gyrolite in the natural sample with that of synthetic gyrolite, Fig. 9 shows the overall habitus of a synthetic sample in which the isometric particles 1—3 μm in size, with certain indications of hexagonal symmetry, are those of gyrolite. A minute content of truscottite with a similar habitus can also be found in the sample. The occurence of fibriform or acicular particles is indicative of the presence of small amount of xonotlite.

Phase transformations of a laumontite-gyrolite sample due to hydrothermal treatment

A sample of natural gyrolite-laumontite with admixtures of stilbite and clinoptilolite (Fig. 10 (1)) in aqueous suspension (solid phase: water = 1 : 10) was subjected to hydrothermal treatment. Its products were as follows: at 200 °C for 7 days:

— gyrolite remains stable and retains its distinct arrangement of the crystalline structure, revealed on the *X*-ray diffraction pattern above all by intensive basal

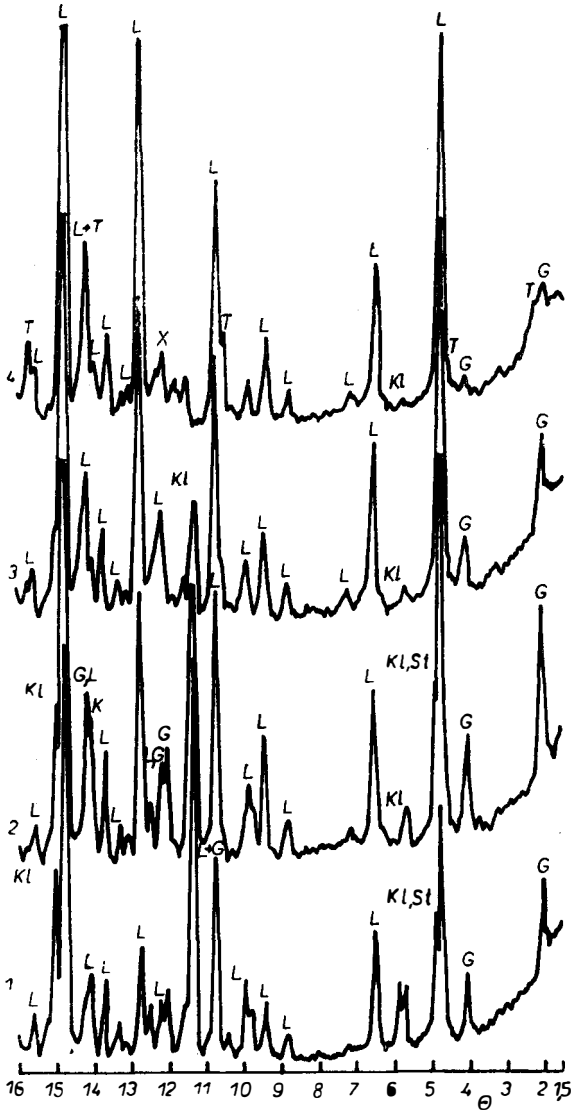

Fig. 10. X-ray diffraction patterns of natural gyrolite with laumontite, original (1) and after hydrothermal treatment at 200 °C (2), 250 °C (3) and 300 °C (4).

Table 1

1		2		3		4		5		6	
V-4 490 m		V-4 490 m		V-6 484 m		V-4 768,2 m		Synthetic gyrolite		Synthetic truscottite	
d nm	I rel	d nm	I rel	d nm	I rel	d nm	I rel	d nm	I rel	d nm	I rel
2.20	8	2.20	5	2.138	1			2.20	8		
1.90	1									1.948	8
1.10	6	1.10	10	1.130	1			1.10	6		
0.938	10	0.945	10	0.938	10	0.966	10			0.960	10
0.906	6	0.918	5			0.914	10				
0.752	8	0.760	3					0.779	1	0.760	2
0.679	6	0.683	6	0.679	10	0.696	8				
0.630	1			0.613	3	0.616	1			0.629	4
0.501	3			0.500	3	0.509	2				
0.471	5	0.471	3	0.467	4	0.476	6			0.468	3
0.452	2D					0.452	1	0.468	1		
0.448	2D	0.443	1	0.444	3	0.434	1				
0.426	2	0.426	1								
0.413	6	0.414	3	0.412	10	0.418	8	0.417	5	0.415	8
0.392	10	0.393	10			0.399	1			0.402	4
0.384	1			0.381	3	0.388	1	0.380	2		
0.378	3	0.379	1	0.372	1	0.377	1			0.379	3D
0.370	5	0.369	3							0.371	6
0.364	1			0.363	5	0.368	1	0.368	3		
0.349	4	0.349	2	0.348	8	0.351	3	0.349	1	0.347	2
0.339	1			0.338	2						
0.334	1										
0.332	1			0.332	3						
0.325	3	0.325	3	0.324	5	0.327	3				
0.316	5	0.313	3	0.312	3D	0.315	3	0.314	1	0.312	5
0.303	10	0.302	10	0.301	10	0.304	8	0.307	5		
0.286	2	0.286	1	0.285	3	0.288	1			0.284	3
0.282	1			0.282	2			0.281	5		
0.277	1			0.278	2D	0.279	1	0.278	2		
0.266	1	0.266	1			0.267	1	0.266	1	0.262	5
0.256	2	0.256	1	0.255	3	0.256	2				
0.248	4	0.247	1	0.248	2					0.249	2
0.242	4			0.242	3	0.243	1	0.241	2	0.242	2
0.234	3	0.235	1	0.230	2	0.235	2	0.232	1	0.231	1
0.227	2	0.227	1	0.226	3	0.226	1	0.225	1		
0.220	1			0.219	1					0.222	3
0.217	1	0.217	1	0.216	1	0.217	1	0.217	1		
0.214	2	0.214	1	0.213	2	0.214	1				
0.208	3	0.208	1	0.208	3	0.209	1	0.208	2	0.207	1
0.195	1	0.194	1	0.197	1	0.195	1			0.196	1
0.190	4	0.190	2	0.190	5	0.190	1			0.190	1
0.187	2	0.187	1	0.186	3	0.186	1				
0.181	3			0.184	1			0.182	8	0.182	5
0.176	1					0.177	1	0.179	1	0.179	2
0.169	1									0.173	2
0.161	2			0.162	1	0.163	1				
0.157	3	0.157	1	0.159	1	0.157	1	0.157	2		
0.151	2	0.153	1	0.151	2	0.151	1	0.150	1		

1 — Vysoká—Šementlov, fissure fill in granodioric porphyries, powdered 2 — as sample 1, oriented 3 — Vysoká—Šementlov, fissure fill in amphibolic chloritized andesites, oriented 4 — Vysoká—Šementlov, fissure fill in strongly metamorphic granodioritic porphyry, oriented 5 — synthetic gyrolite, oriented 6 — synthetic truscottite, oriented 7 — Mackay, Taylor (1953) 8 —

7		8		9		10		11		12		13	
Tabulated gyrolite		Tabulated gyrolite		Tabulated truscottite		Tabulated truscottite		Tabulated truscottite		Tabulated laumontite		Tabulated laumontite	
d nm	I rel	d nm	I rel	d nm	I rel	d nm	I rel	d nm	I rel	d nm	I rel	d nm	I rel
2.20	10												
				1.90	s	1.90	8	1.90	10				
1.10	8												
		0.960	6	0.940	s	0.940	4	0.948	10	0.949	10	0.942	vs
0.740	4D	0.790	4	0.765	ft	0.778	3	0.773	2				
0.540	2D									0.686	3	0.681	s
		0.640	4	0.630	ft	0.611	3	0.631	3	0.619	1	0.620	ft
				0.502	vft			0.505	1			0.504	ft
0.475	3	0.468	4	0.465	ft	0.465	3	0.472	4	0.473	2	0.473	vft
										0.450	1		
										0.431	1	0.446	ft
0.420	8	0.424	8			0.423	8						
				0.413	s			0.411	2	0.415	6	0.416	vs
		0.384	6	0.380	ft	0.385	4	0.384	4				
						0.378	4	0.376	4	0.376	1		
0.372	2D			0.371	ft								
0.365	6									0.366	1	0.367	vft
		0.354	4	0.347	ft	0.347	4	0.350	4	0.351	3	0.349	s
		0.336	10					0.344	1	0.341	1		
										0.336	1		
												0.332	s
0.321	4D									0.327	2	0.320	vft
0.312	10	0.315	6	0.314	s	0.312	10	0.314	10	0.315	2		
		0.302	2	0.300	s	0.302	2	0.301	3	0.303	3	0.302	ft
		0.392	2	0.283	s	0.282	6	0.284	10	0.288	2	0.287	ft
0.280	4	0.285	8										
0.280	6D									0.279	1	0.277	ft
0.261	6D	0.265	6	0.263	s	0.263	4	0.269	10	0.263	1		
		0.258	2			0.251	1	0.264	8	0.257	2	0.256	vft
		0.245	4	0.249	vft			0.252	1	0.246	1	0.252	vft
0.242	2			0.242	ft	0.242	1	0.243	1	0.244	2	0.242	ft
0.231	2					0.233	1			0.236	1	0.234	ft
		0.229	4	0.226	ft					0.227	1	0.227	ft
		0.225	6	0.223	ft	0.221	3D			0.221	1		
0.217	2	0.212	4							0.215	2	0.215	ft
0.206	2	0.209	4	0.208	ft	0.209	2	0.209	1	0.208	1	0.206	vft
		0.199	2	0.204	ft	0.204	2	0.205	2	0.199	1	0.197	vft
		0.194	2	0.192	ft	0.191	1					0.195	ft
		0.188	8	0.189	ft	0.188	1			0.188	1	0.186	vft
0.182	8	0.181	6	0.183	s	0.183	6	0.183	4			0.181	ft
0.173	1			0,176	ft	0.176	2	0.176	2			0.174	vft
				0.171	vft	0.171	1	0.171	1			0.165	vft
				0.165	ft	0.164	2	0.169	1			0.161	ft
0.157	3			0.158	ft	0.159	2	0.161	1			0.153	ft
0.152	2			0.150	ft	0.151	2	0.151	2			0.151	ft

Micheyev (1957) 9 — Mackay, Taylor (1954) 10 — Chalmers et al. (1954), Selected powder diffraction data of minerals (1974), 17, 761 11 — Selected powder diffraction data of minerals (1974), 19, 229 12 — Breck (1974) 13 — Deer, Howie, Zussman (1963); vs — very strong, s — strong, ft — faint, vft — very faint

diffractions at 2.2 and 1.1 nm, while the other minerals remain unchanged (Fig. 10 (2)); at 250 °C for 7 days:

— the phase composition of the initial material already shows changes revealed by a marked decrease of the gyrolite diffractions intensity, while the presence os laumontite and the other minerals remains uncharged (Fig. 10 (3)). Gyrolite it already becoming unstable in agreement with the literary data [8, 11, 12]; at 300 °C for 7 days:

— only minute amounts of metastable gyrolite remain, and truscottite and xonotlite with diffractions of generally low intensity begin to form, occurring in mixture with stable laumontite. The stilbite and clinoptitolite phases have disappeared (Fig. 10 (4)).

The course of thermal decomposition of gyrolite and laumontite in the natural sample after hydrothermal treatment at 200, 250 and 300 °C is shown by DSC curves (1—3) in Fig. 4. Except for the decomposition of calcite over the temperature range of 600 to 800 °C, the other thermal effects are attributed to dehydration and dehydroxidation of gyrolite and laumontite. The dehydration of gyrolite is revealed by the distinct endotherm at 100—120 °C and its dehydroxidation by the endotherm at 415 °C (the DSC curves *1* and *2*). The course of dehydration and dehydroxidation of synthetic gyrolite in comparison with natural gyrolite is analogous; however, the thermoeffect on the DSC curves is associated with more pronounced losses in weight and over a wider temperature range. The difference may be related to particle sizes, or their dispersity and structural arrangement. The dehydration of laumontite (DSC curve 3) in the range of 100 °C corresponds to liberation of water bound physically on the surface of crystals. The endeffect over the temperature interval of 120 to 260 °C corresponds to dehydration of zeolite laumontite which produces wairakite [20, 21]

$$CaAl_2Si_4O_{12} \cdot 4\,H_2O \;=\; CaAl_2Si_4O_{12} \cdot 2\,H_2O + 2\,H_2O$$

The endotherm between 250 and 300 °C conforms to the dehydration of wairakite. Following isothermal heating of the natural samples for 1 hour at 300 °C, the basal diffractions of gyrolite faded out, disappearing completely at 400 °C. The isothermal heating shows that due to dehydration and dehydroxidation, the periodicity of layers in the structure is gradually impaired in the direction of crystallographic axis **Z**, which leads to its decomposition.

Formation and stability of synthetic gyrolite during the hydrothermal process

The formation and stability of synthetic gyrolite was studied under hydrothermal conditions at 200, 250 and 300 °C in an aqueous suspension of the mixture CaO and SiO_2 (solid phase: water = 1 : 10) with the molar ratio $CaO/SiO_2 = 0.66$. The phase products obtained by the hydrothermal reactions of the mixture were identified by *X*-ray diffraction analysis by means of ASTM data, and by IR spectroscopy according to the data listed in Table II.

The conditions and formation of the products of variable thermal syntheses of the gyrolite mixture $CaO/SiO_2 = 0.66$ are as follows:

isothermal heating at 200 °C for 7 days

Table II

Characteristic wave numbers γ in cm^{-1} of gyrolite, truscottite, xonotlite and cristobalite [23, 24, 25]

Gyrolite	Truscottite	Xonotlite	Cristobalite
390	645	413	470
465	825	465	516
480	955	546	695
500	990	612	785
600	1010	635	802
610	1080	672	1100
675	1100	928	1178
785	1150	975	
1000	1280	1010	
1030		1070	
1125		1200	

— the phase composition of the products consists mostly of gyrolite with a small share of xonotlite

isothermal heating at 250 °C for 7 days

— the product contains a mixture of gyrolitic phases and a minute amount of truscottite and xonotlite

isothermal heating at 200 °C for 7 days and subsequent heating at 250 °C for 7 days

— the phases present are metastable gyrolite and a small amount of forming stable truscottite. The comparatively distinct diffraction at 0.262 nm corresponds to gyrolite, even through this is specified by Harker [12] for natural gyrolite only. The typical more diffuse profile of the pronounced diffraction with a maximum at 0.313 nm is likewise typical for gyrolite

isothermal heating at 200 °C for 7 days and subsequent heating at 300 °C for 7 days:

— in the product, gyrolite was completely converted to truscottite and xonotlite. The results obtained are in agreement with the data on the equilibrium and stability of phases given by Luke and Taylor [22].

The conversion of truscottite to gyrolite+cristobalite over the temperature range of 300—200 °C was studied on an aqueous suspension in a mixture having the molar ratio $CaO/SiO_2 = 0.50$. Following hydrothermal treatment at 300 °C for 7 days, the product contained truscottite as the main phase, with a minute admixture of xonotlite and cristobalite. The phase association was again submitted to hydrothermal treatment with isothermal heating at the reduced temperature of 200 °C (7 days). However, under these conditions the expected conversion of truscottite to gyrolite+cristobalite did not take place, probably owing to a kinetic barrier associated with the activation energy of the process.

A comparison of the products of the syntheses and the decomposition over the temperature range of 200 to 300 °C shows that gyrolite was formed and stabilized at 200 °C. Above this temperature, it already becomes unstable, being decomposed

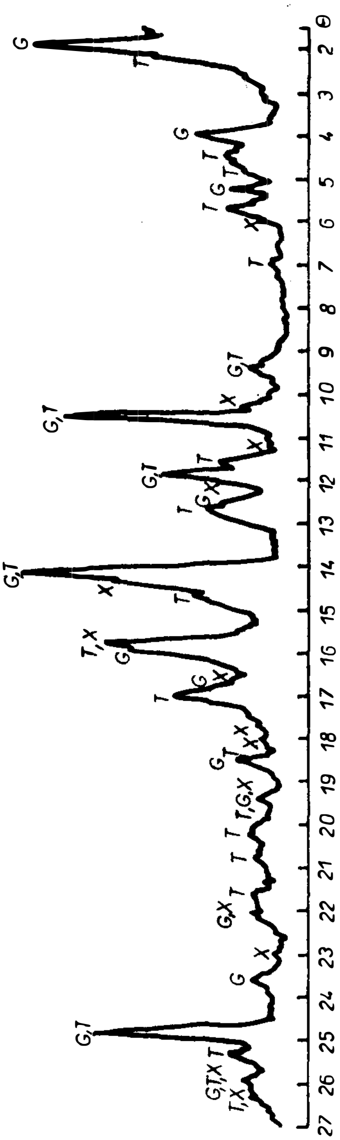

Fig. 11. X-ray diffraction pattern of the products of synthetic gyrolite (prepared at 200 °C) after hydrothermal treatment at 250 °C.

to stable hydrates truscottite and xonotlite according to the reaction $6\ C_2S_3H_2 \rightarrow$ $\rightarrow 3\ C_2S_4H + C_6S_6H + 8\ H_2O$. The decomposition process of gyrolite with subsequent formation of the stable hydrates truscottite and xonotlite is proved by the inequilibrium phase association gyrolite+truscottite+xonotlite, obtained at 250 °C (7 days) in which, however, gyrolite acts as a metastable phase (Fig. 11 and Fig 12). The phase association truscottite+tobermorite, stable at about 250 °C [12], was not established in this experiment. Apart from gyrolite, truscottite and xonotlite, cristobalite was also found in some of the experiments. Luke and Taylor [22] point out that the phase composition or a different molar ratio CaO/SiO_2 of the product in various layers of the hydrated specimen, studied in the pressure cylinder, may be affected by the influence of various parameters and random effects (e.g. the temperature and concentration gradients, inhomogeneity of the mixture, the form and dispersity of SiO_2, and others).

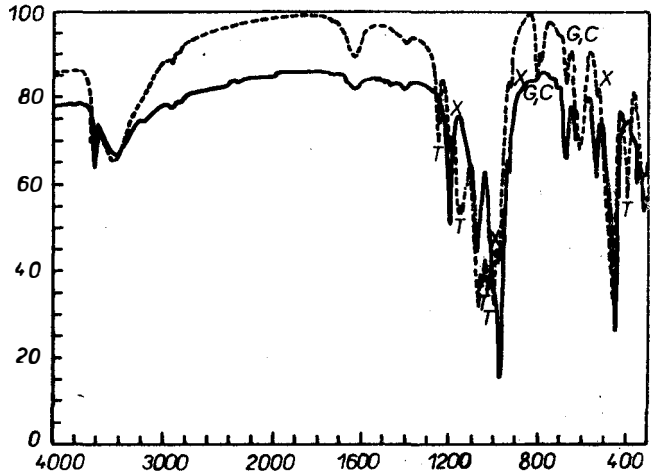

Fig. 12. IR absorption spectra of the products of synthetic gyrolite (prepared at 200 °C) following hydrothermal treatment at 250 °C (- -) and the products after direct synthesis at 250 °C (——).
Note: All the minerals are designated by the following abbreviations: gyrolite G, laumontite L, truscottite T, xonotlite X, cristobalite C, calcite K, stilbite St, clinoptilolite Kl.

CONCLUSION

1. The morphological, crystallographical and mineralogical properties of the natural sample were studied and some of its mineralogical characteristics established. In paragenesis, the natural sample contains gyrolite and laumontite as the main phase association, with a small admixture of zeolitic minerals stilbite and clinoptilolite.

2. The stability and products of the decomposition process of natural gyrolite in association with laumontite were compared with those of synthetic gyrolite over the temperature range of 200 to 300 °C under the pressure of saturated water vapour. Both natural and synthetic gyrolite were found to behave analogously under hydrothermal conditions. At 200 °C, gyrolite is a stable phase co-existing

with laumontite. Above this temperature, both natural and synthetic gyrolite decompose, forming the stable phases truscottite and xonotlite. A stable phase association of truscottite+xonotlite+laumontite exists over the temperature range of 250 to 300 °C.

References

[1] Harman M., Horváth I., Števula L., Petr K.: Mineralia Slovaca *21*, 357, (1989).
[2] Kratochvíl J.: *Topographic Mineralogy of Bohemia I.—VIII.*, Prague 1957—64.
[3] Mackay A. L., Taylor H. F. W.: Mineralogical Magazine *30*, 80 (1953).
[4] Chalmers R. A., Farmer V. C., Harker R. I., Kelly S., Taylor H. F. W.: Mineralogical Magazine *33*, 831 (1964).
[5] Merlino S.: Nature *238*, 124 (1972).
[6] Gard J. A., Mitsuda T., Taylor H. F. W.: Mineralogical Magazine *40*, 325 (1975).
[7] Lachowski E. E., Murray L. W., Taylor H. F. W.: Mineralogical Magazine *43*, 333 (1979).
[8] Taylor H. F. W.: *The Chemistry of Cements*, Vol. I. p. 168, Academic Press, London and New York 1964.
[9] Roy D. M., Harker R. I.: *Proceedings of the Fourth International Symposium on the Chemistry of Cement*, Vol. I, p. 196, Washington 1960.
[10] Harker R. I.: Journal of the American Ceramic Society *47*, 521 (1964).
[11] Kalousek G. L., Nelson E. B.: Cement and Concrete Research *8*, 283 (1978).
[12] Števula L., Petrovič J.: Cement and Concrete Research *13*, 684 (1983).
[13] Breck D.: *Zeolite Molecular Sieves*, Structure, Chemistry and Use p. 158. Wiley, London 1974.
[14] Micheiev V. I.: *X-Ray Classification of Minerals* (in Russian) 1957.
[15] Mackay A. L., Taylor H. F. W.: Mineralogical Magazine *30*, 450 (1954).
[16] ibid [4].
[17] *Selected Powder Diffraction Data for Minerals*. Publ. OBM, 1—23, Philadelphia 1974.
[18] ibid. [13].
[19] Deer W. A., Howie R. A., Zussman J.: *Rock Forming Minerals*, Vol. 4. Longmans, London 1963.
[20] Thompson A. B.: Amer. Journ. Sci. *269*, 267 (1970).
[21] Liou J. G.: Journal of Petrology *12*, 379 (1971).
[22] Luke K., Taylor H. F. W.: Cement and Concrete Research *14*, 657 (1984).
[23] Speakman K.: Mineralogical Magazine *36*, 1090 (1968).
[24] Moenke H.: *Mineralspektren II.*, Akademie Verlag, Berlin 1966.
[25] Hlavay J., Jones K., Elek S., Inczedy J.: Clays and Clay Minerals *26*, 139 (1978).

MINERÁL GYROLIT A JEHO STABILITA ZA HYDROTERMÁLNYCH PODMIENOK

Ladislav Števula, Miroslav Harman*, Ivan Horváth, Karol Putyera

Ústav anorganickej chémie Centra chemického výskumu Slovenskej akadémie vied, Dúbravská cesta, 842 36 Bratislava

**Geologický ústav Centra geovedného výskumu Slovenskej akadémie vied, Dúbravská cesta 814 73 Bratislava*

Minerál gyrolit nájdený prvý krát na Slovensku (v lokalite Banisko) v paragenéze s laumontitom sa podrobil vo vodnej suspenzii hydrotermálnemu procesu pri 200 °C, 250 °C a 300 °C za účelom sledovania a porovnania jeho stability so syntetickým gyrolitom.

Produkty hydrotermálnej reakcie a ich vlastnosti sa sledovali rtg. difrakčnou analýzou, termickými metódami, IČ absorpčnou spektroskopiou a rastrovacou elektrónovou mikroskópiou.

Zistilo sa, že za relatívne nízkeho tlaku (v rozsahu 1,53—8,48 MPa) v prostredí nasýtenej vodnej pary prírodný gyrolit zostáva pomerne stály maximálne do 250 °C. Pri ďalšom zvyšovaní

teploty do 300 °C postupne prechádza na truscottit, pričom laumontit zostáva pomerne stabilný. Syntetický gyrolit ako porovnávacia vzorka pripravená za hydrotermálnych podmienok pri 200 °C, sa pri 300 °C mení na truscottit a xonotlit.

Obr. 1. Rovnovážny fázový diagram v sústave $CaO—SiO_2—H_2O$ *za hydrotermálnych podmienok pri 200 °C.*

Obr. 2. Rovnovážny fázový diagram v sústave $CaO—SiO_2—H_2O$ *za hydrotermálnych podmienok pri 250 °C.*

Obr. 3. Rovnovážny fázový diagram v sústave $CaO—SiO_2—H_2O$ *za hydrotermálnych podmienok pri 300 °C.*

Obr. 4. Krivky DSC vodnej suspenzie prírodnej vzorky po hydrotermálnom procese pri 200 °C (krivka 1), 250 °C (krivka 2) a 300 °C (krivka 3).

Obr. 5. IČ absorpčné spektrum vzorky prírodného gyrolitu s laumontitom.

Obr. 6. Snímka ERM vzorky prírodného gyrolitu.

Obr. 7. Snímka ERM vzorky prírodného laumontitu.

Obr. 8. Snímka ERM vzorky prírodného gyrolitu a laumontitu.

Obr. 9. Snímka ERM vzorky syntetického gyrolitu.

Obr. 10. Rtg. difrakčné záznamy prírodného gyrolitu s laumontitom pôvodného (1) a po hydrotermálnom spracovaní pri 200°C (2), 250°C (3) a 300°C (4).

Obr. 11. Rtg. difrakčný záznam produktov syntetického gyrolitu (pripraveného pri 200 °C) po hydrotermálnom procese pri 250 °C.

Obr. 12. IČ absorpčné spektrá produktov syntetického gyrolitu (pripraveného pri 200 °C) po hydrotermálnom procese pri 250 °C (- - -) a produktov po priamej syntéze pri 250 °C (——).

Poznámky: Všetky minerály označené skratkami : gyrolit-G, laumontit-L, truscottit-T, xonotlit-X, cristobalit-C, kalcit-K, stilbit-St, klinoptilolit-Kl.

МИНЕРАЛ ГИРОЛИТ И ЕГО УСТОЙЧИВОСТЬ ПРИ ГИДРОТЕРМИЧЕСКИХ УСЛОВИЯХ

Ладислав Штевула, Мирослав Гарман*, Иван Горват, Карол Путьера

Институт неорганической химии Центра химического исследования Словацкой академии наук, Дубравска цеста, 842 36 Братислава

**Геологический институт Центра геонаучного исследования Словацкой академии наук, Дубравска цеста, 814 73 Братислава*

Минерал гиролит, найденный в первый раз в Словакии (месторождение Баниско) в парагенезисе с лаумонтитом, подвергали в водной суспензии гиротермическому процессу при температуре 200, 250 и 300° с целью исследования и сопоставления его устойчивости с синтетическим гиролитом.

Продукты гидротермической реакции и их свойства исследовали с помощью ртг. дифракционного анализа, термических методов, ИК абсорбционной спектроскопии и сканирующей электронной микроскопии.

Было установлено, что при относительно низком давлении (в пределах от 1,53 до 8,48 МПа) в среде насыщенного водяного пара природный гиролит остается относительно устойчивым до температуры 250 °С. При дальнейшем повышении температуры до 300 °С постепенно переходит в трускоттит, причем лаумонтит остается относительно устойчивым. Синтетический гиролит в качестве сопоставительного образца, полученного при гидротермических условиях при 200 °С, переходит при температуре 300 °С в трускоттит и ксонотлит.

Рис. 1. Равновесная фазовая диаграмма в системе $CaO—SiO_2—H_2O$ *при гидротермических условиях при температуре 200 °C.*

Рис. 2. Равновесная фазовая диаграмма в системе $CaO—SiO_2—H_2O$ *при гирдротермических условиях при температуре 250 °C.*

Рис. 3. Равновесная фазовая диаграмма в системе $CaO—SiO_2—H_2O$ *при гидротермических условиях при температуре 300 °C.*

Рис. 4. Кривые DSC водной суспензии природного образца после гидротермического процесса при температуре 200 °C (кривая 1), 250 °C (кривая 2) и 300 °C (кривая 3).

Рис. 5. ИК абсорбционный спектр образца природного гиролита с лаумонтитом.

Рис. 6. Съемка ERM образца природного гиролита.

Рис. 7. Съемка ERM образца природного лаумонтита.

Рис. 8. Съемка ERM образца природного гиролита и лаумонтита.

Рис. 9. Съемка ERM образца синтетического гиролита.

Рис. 10. Ртг. дифракционные записи природного гиролита с лаумонтитом исходным (1) и после гидротермической обработки при температуре 200 °C (2), 250 °C (3) и 300 °C (4).

Рис. 11. Ртг. дифракционная запись продуктов синтетического гиролита (приготовленного при 200 °C) после гидротермического процесса при 250 °C.

Рис. 12. ИК абсорбционные спектры продуктов синтетического гиролита (приготовленного при 200 °C) после гидротермического процесса при 250 °C (- - -) и продуктов после непосредственного синтеза при 250 °C (———).

Примечание: Все минералы обозначаются через латинские буквы: гиролит — G, лаумонтит — L, трускоттит — T, ксонотлит — X, кристобалит — C, кальцит — K, стильбит — St, клиноптилолит — Kl.

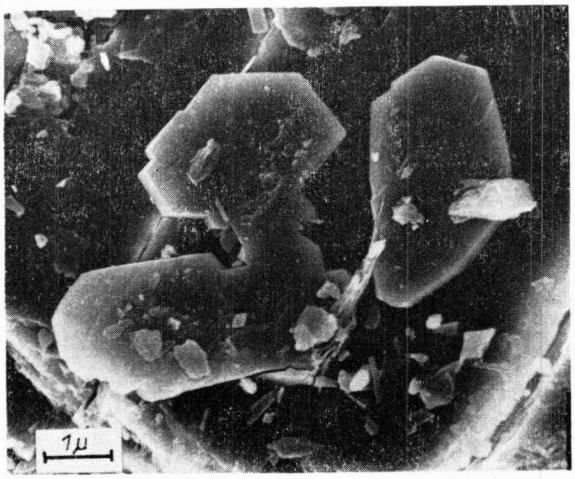

Fig. 6. SE micrograph of a sample of natural gyrolite.

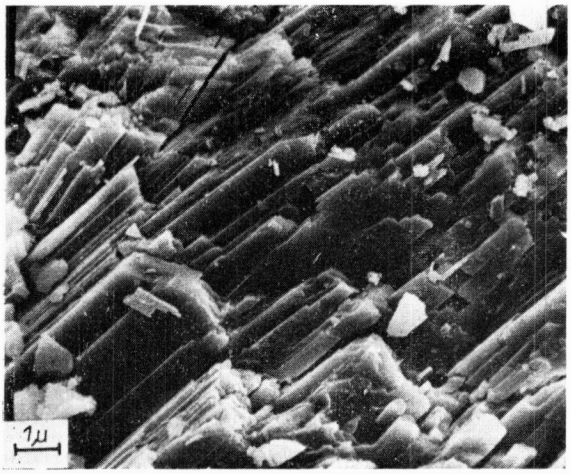

Fig. 7. SE micrograph of a sample of natural laumontite.

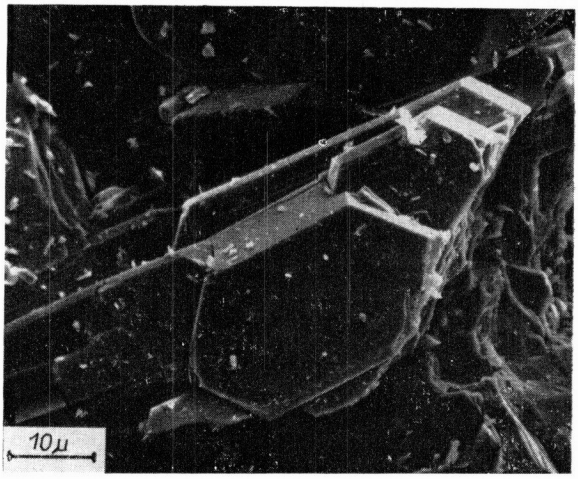

Fig. 8. SE micrograph of a sample of natural gyrolite and laumontite.

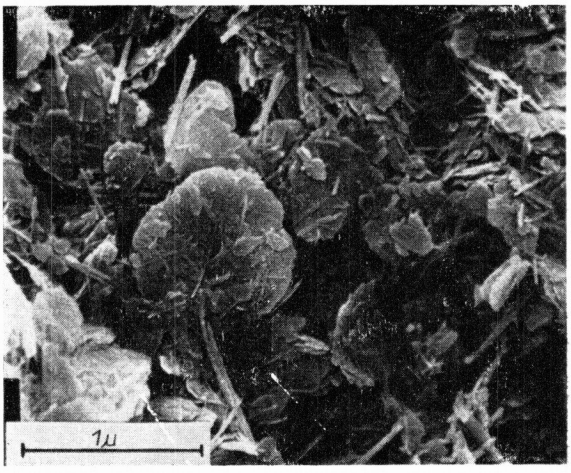

Fig. 9. SE micrograph of a sample of synthetic gyrolite.